Molecular Biology of the Cell
Vol. 8, 2677–2691, December 1997

# *BIM1* Encodes a Microtubule-binding Protein in Yeast

**Katja Schwartz,* Kristy Richards,* and David Botstein†**

Department of Genetics, Stanford University School of Medicine, Stanford, California 94305

Submitted July 14, 1997; Accepted September 15, 1997
Monitoring Editor: J. Richard McIntosh

A previously uncharacterized yeast gene (*YER016w*) that we have named *BIM1* (binding to microtubules) was obtained from a two-hybrid screen of a yeast cDNA library using as bait the entire coding sequence of *TUB1* (encoding α-tubulin). Deletion of *BIM1* results in a strong bilateral karyogamy defect, hypersensitivity to benomyl, and aberrant spindle behavior, all phenotypes associated with mutations affecting microtubules in yeast, and inviability at extreme temperatures (i.e., ≥37°C or ≤14°C). Overexpression of *BIM1* in wild-type cells is lethal. A fusion of Bim1p with green fluorescent protein that complements the *bim1*Δ phenotypes allows visualization in vivo of both intranuclear spindles and extranuclear microtubules in otherwise wild-type cells. A *bim1* deletion displays synthetic lethality with deletion alleles of *bik1*, *num1*, and *bub3* as well as a limited subset of *tub1* conditional-lethal alleles. A systematic study of 51 *tub1* alleles suggests a correlation between specific failure to interact with Bim1p in the two-hybrid assay and synthetic lethality with the *bim1*Δ allele. The sequence of *BIM1* shows substantial similarity to sequences from organisms across the evolutionary spectrum. One of the human homologues, EB1, has been reported previously as binding APC, itself a microtubule-binding protein and the product of a gene implicated in the etiology of human colon cancer.

## INTRODUCTION

In budding yeast (*Saccharomyces cerevisiae*) the microtubule cytoskeleton has been implicated in a limited number of cellular functions (for a recent review see (Botstein *et al.*, 1997)). In addition to the separation of chromosomes during mitosis, only two other functions clearly have been shown to require intact microtubules: movement of the nucleus to the bud neck just prior to separation of the chromosomes and nuclear fusion (karyogamy) following cellular fusion during mating (Huffaker *et al.*, 1988). Yeast microtubules are always found attached to a spindle pole embedded in the nuclear membrane (Byers, 1981). The intranuclear microtubules project into the nucleus and appear to be responsible for chromosome separation, whereas the extranuclear microtubules have been functionally implicated in both the premitotic nuclear movements and karyogamy (Huffaker *et al.*, 1988).

In most eukaryotic cells, the diversity in function of different types of microtubules in the same cell can be attributed to differences in the tubulin isoforms comprising microtubules or to differences in the bound associated proteins, or both. In *S. cerevisiae*, there is only one gene encoding β-tubulin, and either of the two α-tubulin-encoding genes has repeatedly been shown to suffice for all of the normal microtubule-associated functions (Neff *et al.*, 1983; Schatz *et al.*, 1986, 1988). Thus, it appears that the basis for the diversity of functions must lie in the associated proteins and not in the tubulin polymer itself. For this reason, searches for authentic microtubule-binding proteins have been carried out in yeast for many years, with the resulting discovery of a number of such proteins (Meluh and Rose, 1990; Barnes *et al.*, 1992; Hoyt *et al.*, 1992; Roof *et al.*, 1992; Pasqualone and Huffaker, 1994; Interthal *et al.*, 1995; Irminger-Finger *et al.*, 1996; Botstein *et al.*, 1997).

Among these there are several that decorate microtubules when examined in colocalization experiments. Some of these are nonessential for growth, although their absence does produce a phenotype (Hoyt *et al.*, 1992; Roof *et al.*, 1992; Interthal *et al.*, 1995; Pellman *et al.*, 1995). The protein product of the *BIK1* gene is a

* These authors contributed equally to the work.
† Corresponding author.

© 1997 by The American Society for Cell Biology

**Table 1.** Yeast strains used in this study

| Strain | Genotype | Source or Reference |
|---|---|---|
| Y190 | *MAT***a** *gal4 gal80 his3 trp1-901 ade2-101 ura3-52 leu2-3,112 + URA3::GAL-lacZ, LYS2::GAL(UAS)-HIS3 cyh*$^r$ | Bai and Elledge, 1996 |
| DBY4869 | *MATα ura3-52 his4-619 tub2-201* | This laboratory |
| DBY6654 | *MAT***a** *lys2-801 ade2-101 his3-Δ200 leu2-Δ1 ura3-52 TUB1–LEU2* | K. Richards, in preparation |
| DBY6592 | *MATα lys2-801 ade2-101 his3-Δ200 leu2-Δ1 ura3-52 TUB1–LYS2* [*pRB326*] | K. Richards, in preparation |
| DBY7826 | *MATα lys2-801 ade2-101 his3-Δ200 leu2-Δ1 ura3-52 TUB1–LYS2* | This study |
| DBY7306 | *MATα lys2-801 ade2-101 his3-Δ200 leu2-Δ1 ura3-52 TUB1–LEU2* | This study |
| DBY7300 | *MATα lys2-801 ade2-101 his3-Δ200 leu2-Δ1 ura3-52 TUB1–LYS2 bim1Δ::URA3* | This study |
| DBY7301 | *MATα lys2-801 ade2-101 his3-Δ200 leu2-Δ1 ura3-52 TUB1–LYS2 bim1Δ::ura3::ADE2* | This study |
| DBY7303 | *MAT***a** *lys2-801 ade2-101 his3-Δ200 leu2-Δ1 ura3-52 TUB1–LEU2 bim1Δ::ura3::ADE2* | This study |
| DBY7305 | *MATα lys2-801 ade2-101 his3-Δ200 leu2-Δ1 ura3-52 TUB1–LEU2 bim1Δ::ura3::ADE2* | This study |
| DBY7827 | *MATα lys2-801 ade2-101 his3-Δ200 leu2-Δ1 ura3-52 TUB1–LYS2 bik1Δ::ADE2* [*pRB326*] | This study |
| DBY7828 | *MATα lys2-801 ade2-101 his3-Δ200 leu2-Δ1 ura3-52 TUB1–LYS2 num1Δ::URA3* | This study |
| DBY7829 | *MATα lys2-801 ade2-101 his3-Δ200 leu2-Δ1 ura3-52 TUB1–LYS2 bub3Δ::ADE2* [*pRB326*] | This study |
| DBY7830 | *MATα lys2-801 ade2-101 his3-Δ200 leu2-Δ1 ura3-52 TUB1–LYS2 tub2-201* [*pRB326*] | This study |
| DBY7831 | *MATα lys2-801 ade2-101 his3-Δ200 leu2-Δ1 ura3-52 TUB1–LEU2 bik1Δ::ADE2* | This study |
| DBY7832 | *MATα lys2-801 ade2-101 his3-Δ200 leu2-Δ1 ura3-52 TUB1–LYS2 num1Δ::URA3* | This study |
| DBY7833 | *MATα lys2-801 ade2-101 his3-Δ200 leu2-Δ1 ura3-52 TUB1–LEU2 bub3Δ::ADE2* | This study |
| DBY7834 | *MAT***a** *lys2-801 ade2-101 his3-Δ200 leu2-Δ1 ura3-52 TUB1–LYS2 tub3Δ::HIS3 tub2-201* [*pRB326*] | This study |
| DBY7835 | *MAT***a** *lys2-801 ade2-101 his3-Δ200 leu2-Δ1 ura3-52 TUB1–LYS2 bik1Δ::ADE2* | This study |
| DBY7836 | *MAT***a** *lys2-801 ade2-101 his3-Δ200 leu2-Δ1 ura3-52 TUB1–LEU2 num1Δ::URA3* | This study |
| DBY7837 | *MAT***a** *lys2-801 ade2-101 his3-Δ200 leu2-Δ1 ura3-52 TUB1–LYS2 bub3Δ::ADE2* [*pRB326*] | This study |

good example: originally identified serendipitously as a karyogamy-defective mutant, the *bik1* null mutant also was found to have more subtle defects in spindle morphology (Trueheart *et al.*, 1987). However, *bik1* mutants display synthetic lethality with tubulin mutations (Berlin *et al.*, 1990) as well as mutations in other genes. A particularly interesting genetic characteristic of *BIK1* is that overexpression of the gene has a strong phenotype, resulting in the disappearance of microtubule structures and arrest of cell division (Berlin *et al.*, 1990). This suggests that the stoichiometry of Bik1p is somehow important and supports a role for Bik1p in microtubule cytoskeleton structure as well as function.

Here, we characterize another gene encoding a microtubule-binding protein that appears to have a structural and functional role in the microtubule cytoskeleton. This gene (called *BIM1* for binding to microtubules; the open reading frame is YER016w) emerged from a two-hybrid screen in which *TUB1*, the major gene encoding yeast α-tubulin, was used as the "bait." In addition to *BIM1*, the screen identified *TUB2* (encoding β-tubulin) and *BIK1*. We show that Bim1p colocalizes with both intranuclear and extranuclear microtubules; that deletion mutants are viable but have obvious microtubule phenotypes, including a strong bilateral karyogamy defect and synthetic lethality with *tub1* and *bik1* mutations; and that overexpression of *BIM1* results in a readily scorable microtubule phenotype including cell cycle arrest.

Finally, the sequence of *BIM1* is similar to the sequence of human EB1, a putative ligand of APC, the adenomatous polyposis tumor suppressor protein implicated in the etiology of inherited colon cancer (Groden *et al.*, 1991). Human EB1 was originally identified in a two-hybrid screen using APC as bait and the homology to the then uncharacterized YER016w open reading frame was noted (Su *et al.*, 1995). It is particularly interesting that wild-type (but not mutant) APC has been associated both structurally and functionally with the microtubule cytoskeleton in mammalian systems (Munemitsu *et al.*, 1994; Smith *et al.*, 1994). In addition, APC localization depends on intact microtubules (Smith *et al.*, 1994; Nathke *et al.*, 1996). Our findings provide context for these observations.

## MATERIALS AND METHODS

### *Strains and Media*

Yeast strains are listed in Table 1, plasmids in Table 2. Standard methods were used for growth, sporulation, and genetic analysis of yeast (Guthrie and Fink, 1991). Strains DBY7830 and DBY7834 are the products of the *tub2–201* allele from DBY4869 backcrossed six times to DBY6654 or a similar congenic strain.

### *DNA Manipulations and Plasmid Constructions*

DNA cloning was performed using standard methods (Sambrook *et al.*, 1989). Oligonucleotide sequences are listed in Table 3. To construct pRB2510, the *ACT1* terminator was excised from pTS161 as a *Bam*HI-*Sph*I fragment and inserted into *Bam*HI-*Sph*I sites of pRB1508. To construct pRB2514, *TUB1* was amplified by polymerase chain reaction (PCR) from the genomic DNA as a template using Vent polymerase (New England Biolabs, Beverly, MA) and primers TUB1–1 and TUB1–2. The PCR fragment was subsequently digested with *Nco*I and inserted into the *Nco*I site of pRB2510. Mutant *tub1* alleles were amplified using the same primers (except for *tub1–801* which required primer tub1–3, and alleles *tub1–851* and *tub1–852* which required primers tub1–4 and tub1–5, respectively) and cloned into pRB2510 in duplicate. Plasmid pRB2639 was con-

**Table 2.** Plasmids used in this study

| Plasmid | Description | Source or Reference |
|---|---|---|
| pRB1508 | CEN-based *GAL4* DNA-binding domain vector | Amberg *et al*., 1995 |
| pSE 1112 | *SNF1* fused to DNA-binding domain of *GAL4* in pAS2 | Bai and Elledge, 1996 |
| pTS161 | YCp50-based vector with *GAL1-10* promoter and actin terminator | T. Stearns, personal communication |
| pJJ244 | pUC18-based vector containing *URA3* | Jones and Prakash, 1990 |
| pASZ10 | *ADE2*-containing vector | Stotz and Linder, 1990 |
| pRB2138 | GFP (S65T) fusion expression vector | Doyle and Botstein, 1996 |
| pRB326 | *TUB1* in CEN-based vector containing *URA3* | Schatz *et al*., 1986 |
| pRB2510 | CEN-based bait vector with terminator | This study |
| pRB2514 | *TUB1* in pRB2510 | This study |
| pRB2639 | *TUB3* in pRB2510 | This study |
| pRB2637 | *ura3::ADE2* disruption plasmid | This study |
| pRB2654 | GFP-Bim1p fusion plasmid | This study |
| pRB2652 | *BIM1* under *GAL1* promoter | This study |
| pRB2663 | *ADE2* in pUC19 polylinker | This study |

structed similarly to pRB2514, except that primers for *TUB3* amplification were TUB3–1 and TUB3–2. For pRB2637, the *ADE2* gene was excised as a *Bgl*II fragment from pASZ10 (Stotz and Linder, 1990) and blunt-end ligated into the *Eco*RV and *Stu*I sites of pJJ244 (Jones and Prakash, 1990). To make pRB2654, *BIM1*, amplified by PCR with Vent polymerase and primers BIM1–1 and BIM1–2, was digested with *Bam*HI and *Xba*I and cloned into the *Bam*HI and *Xba*I sites of pRB2138. To construct pRB2652, the same PCR product as for pRB2654 was inserted into the *Bam*HI and *Xba*I sites of pTS161. pRB2663 was constructed by inserting the *Bgl*II fragment from pASZ10 (Stotz and Linder, 1990), containing the *ADE2* gene, into the *Bam*HI site of pUC19 (Sambrook *et al*., 1989).

## *Gene Disruptions*

Disruptions were constructed by double-fusion PCR (Amberg *et al*., 1995b). The *bim1Δ::URA3* allele was created using primers bim1Δ-1, bim1Δ-2, bim1Δ-3, and bim1Δ-4. The *URA3* marker was amplified by using plasmid pJJ242 (Jones and Prakash, 1990) as a template and M13 "forward" and "reverse" primers. Since such deletions are

**Table 3.** Sequences of the oligonucleotides

| Oligonucleotide | Sequence |
|---|---|
| TUB1-1 | 5′-CCGCCATGGAGATGAGAGAAGTTATTAGT-3′ |
| TUB1-2 | 5′-GCGCCATGGTTAAAATTCCTCTTCCTC-3′ |
| tub1-3 | 5′-CCGCCATGGAGATGGCTGCAGTTATTAGT-3′ |
| tub1-4 | 5′-GCGCCATGGTTAAAATGCCGCTGCAGC-3′ |
| tub1-5 | 5′-GCGCCATGGTTAAGCTTCCTCTTCCTC-3′ |
| TUB3-1 | 5′-CCGCCATGGAGATGAGAGAGGTCATTAGT-3′ |
| TUB3-2 | 5′-GCGCCATGGTTAGAACTCCTCAGCGTA-3′ |
| BIM1-1 | 5′-CGCGGATCCATGAGTGCGGGTATCGGA-3′ |
| BIM1-2 | 5′-GCGTCTAGATTAAAAAGTTTCCTCGTCGATGATCAGTTG-3′ |
| bim1Δ-1 | 5′-GAGGCATCTTCTTACCTG-3′ |
| bim1Δ-2 | 5′-GTCGTGACTGGGAAAACCCTGGCGCCCGCACTCATTGCTTCG-3′ |
| bim1Δ-3 | 5′-TCCTGTGTGAAATTGTTATCCGCTGGTGAGGTTGGCGTGAGC-3′ |
| bim1Δ-4 | 5′-CGAACCGCCTGAGGCACC-3′ |
| M13 forward | 5′-CGCCAGGGTTTTCCCAGTCACGAC-3′ |
| M13 reverse | 5′-AGCGGATAACAATTTCACACAGGA-3′ |
| bik1Δ-1 | 5′-GGGGTTCGACTGAGCTGCGG-3′ |
| bik1Δ-2 | 5′-GTCGTGACTGGGAAAACCCTGGCGCGCATACACAGCCAGCCACAGC-3′ |
| bik1Δ-3 | 5′-TCCTGTGTGAAATTGTTATCCGCTCCAGCAGTTCTTCTAGGCAGTCG-3′ |
| bik1Δ-4 | 5′-CGAGCCATCCAAAAGTACCTGACC-3′ |
| num1Δ-1 | 5′-CCGAGCCCTGTAGTAGAATGGTGC-3′ |
| num1Δ-2 | 5′-GTCGTGACTGGGAAAACCCTGGCGCGAACGTCTCGTGGAAAGCC-3′ |
| num1Δ-3 | 5′-TCCTGTGTGAAATTGTTATCCGCTGCCGATCATTTGGCAATTTACG-3′ |
| num1Δ-4 | 5′-GCAAAGGATGACTTGGTAGTCGG-3′ |
| bub3Δ-1 | 5′-GTCACCAGAAAACTCCAGTGAGG-3′ |
| bub3Δ-2 | 5′-GTCGTGACTGGGAAAACCCTGGCGGCCGCGACTGTTGTGTTTTCG-3′ |
| bub3Δ-3 | 5′-TCCTGTGTGAAATTGTTATCCGCTCGTGTAGTATGATAGAACATTCC-3′ |
| bub3Δ-4 | 5′-CCTTAGCGGTAAATGCAGCG-3′ |
| 2-H1 | 5′-TGATGAAGATACCCCACC-3′ |
| TUB2-1 | 5′-GTGGAGCACCAAAATCGCC-3′ |

viable (see below), the *bim1*Δ*::URA3* disruption cassette was introduced directly into the haploid DBY7826 (a derivative of DBY6592 that no longer contains pRB326) by transformation, producing DBY7300. For the purpose of genetic analysis, the *bim1*Δ*::ura3::ADE2* allele was created by transforming DBY7300 with the *Sma*I-*Pst*I fragment from pRB2637, producing DBY7301. Strains DBY7303, DBY7305, and DBY7306 were progeny of DBY7301 mated to DBY6654.

The *bik1*Δ*::ADE2* allele was created using primers bik1Δ-1, bik1Δ-2, bik1Δ-3, and bik1Δ-4. The *ADE2* marker was amplified by using plasmid pRB2663 as a template and M13 forward and reverse primers (as above). Since such deletions are viable, the *bik1*Δ*::ADE2* disruption cassette was introduced directly into the haploid DBY6592 by transformation, producing DBY7827.

The *num1*Δ*::URA3* allele was created using primers num1Δ-1, num1Δ-2, num1Δ-3, and num1Δ-4. The *URA3* marker was amplified by using plasmid pJJ242 (Jones and Prakash, 1990) as a template and M13 forward and reverse primers (as above). Since such deletions are viable, the *num1*Δ*::URA3* disruption cassette was introduced directly into the haploid DBY7826 by transformation, producing DBY7828.

The *bub3*Δ*::ADE2* allele was created using primers bub3Δ-1, bub3Δ-2, bub3Δ-3, and bub3Δ-4. The *ADE2* marker was amplified by using plasmid pRB2663 as a template and M13 forward and reverse primers (as above). Since such deletions are viable, the *bub3*Δ*::ADE2* disruption cassette was introduced directly into the haploid DBY6592 by transformation, producing DBY7829.

## *Construction of Double Mutants*

To construct double mutants between *bim1*Δ and the charged-to-alanine *tub1* alleles (Richards, 1997), DBY7301 was crossed to all of the strains listed in Table 4. Diploids were selected using complementing auxotrophic markers and then were sporulated and dissected. In most cases, the strains carried pRB326, containing the wild-type *TUB1* gene; therefore, before analyzing the double-mutant phenotype, cells that had lost the plasmid were selected by growth on 5-fluoroorotic acid.

To construct pairwise combinations of the microtubule cytoskeleton mutants (*bim1*Δ, *bik1*Δ, *num1*Δ, *bub3*Δ, and *tub2–201*), the following MAT**a** strains: DBY7303, DBY7835, DBY7836, DBY7837, and DBY7834 were crossed in all combinations to the following MAT$\alpha$ strains: DBY7301, DBY7831, DBY7832, DBY7833, and DBY7830. In the cases of the *bik1*Δ, *num1*Δ, and *bub3*Δ strains, the parental strains listed were obtained as haploid segregants from a cross between each of the original disruption strains (i.e., DBY7827, DBY7828, and DBY7829, respectively) and DBY6816.

Strains were mated on YPD medium and then zygotes were micromanipulated, each to a distinct spot on the plate, and allowed to form diploid colonies. The diploids were then sporulated and dissected. In the cases where one or both parental strains contained the *TUB1* plasmid pRB326, the plasmid was either eliminated before the cross was made or after the spores germinated. In either case, pRB326 was never present when the phenotypes of the double mutants were scored. Double mutants were identified in any of three ways. In some cases, there were two different auxotrophies marking the two mutants (e.g. *num1*Δ*::URA3 bik1::ADE2* double mutants). In some cases, the phenotypes of the two single mutants were both easily identifiable in the double mutant (e.g., *tub2–201 bim1*Δ mutants acquired the benomyl resistance conferred by *tub2–201* and the temperature sensitivity conferred by *bim1*Δ). Finally, in cases where the parental phenotypes were similar and the auxotrophic markers which marked the two mutants were identical (e.g., *bim1*Δ *bik1*Δ double mutants), the double mutants were identified by segregation analysis. For example, in the case of the *bim1*Δ $\times$ *bik1*Δ cross, the two Ade$^+$ spores in nonparental ditype tetrads were identified as double mutants.

**Table 4.** *tub1* strains used to construct the double mutants with *bim1*Δ[a]

| DBY | *tub1* allele | Amino Acid Changes |
|---|---|---|
| 6654 | 800 | None (wild-type) |
| 6656 | 801 | R2A, E3A |
| 6660 | 803 | K31A, D33A |
| 6662 | 804 | H35A, E37A, D38A |
| 6664 | 805 | K42A, K44A |
| 6666 | 806 | E47A, E48A |
| 6668 | 807 | H55A, E56A |
| 6672 | 809 | D70A, E72A |
| 6674 | 810 | D77A, E78A, R80A |
| 6676 | 811 | K85A, D86A |
| 6678 | 812 | H89A, E91A |
| 6680 | 813 | K97A, E98A, D99A |
| 6682 | 814 | R106A, H108A |
| 6684 | 815 | R113A, E114A |
| 6686 | 816 | D118A, D121A, R122A |
| 6688 | 817 | R124A, K125A |
| 6690 | 818 | D128A, D131A |
| 6692 | 819 | T146A |
| 6696 | 821 | E161A, K164A, K165A |
| 6698 | 822 | K167A, E169A |
| 6702 | 824 | D206A, E208A |
| 6704 | 825 | D212A, K215A, R216A |
| 6706 | 826 | D219A, R222A |
| 6708 | 827 | R244A, D146A |
| 6712 | 829 | R265A, H267A |
| 6714 | 830 | K279A, K281A |
| 6716 | 831 | H284A, E285A |
| 6718 | 832 | K305A, D307A |
| 6720 | 833 | R309A, D310A, K312A |
| 6722 | 834 | R321A, D323A |
| 6724 | 835 | R327A, D328A, R331A |
| 6726 | 836 | E334A, K337A |
| 6728 | 837 | K339A, K340A |
| 6730 | 838 | D373A, R374A |
| 6732 | 839 | E387A, K390A, R391A |
| 6736 | 841 | D393A, R394A |
| 6738 | 842 | K395A, D397A |
| 6744 | 845 | K402A, R403A |
| 6746 | 846 | E412A, E415A |
| 6748 | 847 | E416A, E418A |
| 6750 | 848 | E421A, R423A, E424A, D425A |
| 6752 | 849 | E430A, R431A, D432A |
| 6754 | 850 | E435A, D439A |
| 6756 | 851 | E443A, E444A, E445A, E446A |
| 6758 | 852 | F447A |
| 6760 | 853 | E183A |

[a] All are identical to DBY6654 (see Table 1), except for the presence of the corresponding *tub1* allele indicated in the second column and described in the third column. In most cases, the *tub1* parental strains were also carrying pRB326, but this plasmid was eliminated (by growth on 5-fluoroorotic acid) before analyzing the phenotype of the *bim1*Δ *tub1* double mutants.

## *Two-Hybrid Screen*

Expression of the *GAL4-TUB1* fusion in strain Y190 (transformed with pRB2514) was confirmed by Western blot analysis (Harlow and Lane, 1988) using the anti-hemagglutinin epitope tag antibody 12CA5 (BabCo, Berkeley, CA), diluted 1:1000. Total yeast protein preparation was done as described (Yaffe *et al.*, 1985). The λYES cDNA library was amplified as described (Amberg *et al.*, 1995a).

For the screen itself, strain Y190 containing pRB2514 was transformed with library DNA using the lithium acetate method (Ito *et al.*, 1983) and plated on minimal medium (SD) + 10 $\mu$g/ml adenine and 50 mM 3-amino-1,2,4-triazole (Sigma, St. Louis, MO). The plates were incubated at 25°C for 10 d. In total, $2.6 \times 10^4$ transformants were screened. $\beta$-Galactosidase activity was assayed as described (Bai and Elledge, 1996). Specificity and reproducibility were tested by cotransformation of strain Y190 with library isolates and pRB2514 or pSE1112 (Bai and Elledge, 1996).

Since in preliminary tests *TUB2* had been found to bind *TUB1* in the two-hybrid system, inserts recovered here were screened for the presence of *TUB2* by PCR using one primer corresponding to the vector sequence 2-H1 (Amberg *et al.*, 1995a) and the other a *TUB2* internal primer TUB2–1. Double-stranded dideoxy sequencing was performed with the Sequenase reagent kit (United States Biochemical, Cleveland, OH) using the above vector primer 2-H1.

### *Differential Interaction Screen*

Strain Y190 was cotransformed with *tub1* alanine scan alleles fused to the DNA-binding domain of *GAL4* in pRB2510 (made from duplicate PCR constructs, as above) and *BIM1* or *BIK1* fused to the activation domain of *GAL4* as isolated from the cDNA library. Transformants were selected on minimal medium lacking tryptophan and leucine and then patched or spotted onto minimal medium containing 10 $\mu$g/ml adenine and 50 mM 3-amino-1,2,4-triazole. Positive interaction was confirmed, as above, using the $\beta$-galactosidase assay.

### *Microscopy*

Immunofluorescent staining of yeast was performed using a modification of the methods of Kilmartin and Adams (1984). Cells were fixed in 3.7% formaldehyde in 0.1 M potassium phosphate buffer (pH 6.5) for 60 min at room temperature and washed in 0.1 M potassium phosphate buffer (pH 6.5) and then in 0.1 M potassium phosphate buffer with 1.2 M sorbitol (pH 6.5) and digested with 0.6 mg/ml Zymolyase 100T (ICN ImmunoBiologicals, Costa Mesa, CA). Cells were applied to the wells of multiwell microscope slides coated with 0.1% polylysine (>400,000 molecular weight, Sigma). Subsequent antibody incubations and washes were performed in phosphate-buffered saline (pH 7.4) with 0.5% bovine serum albumin, 0.5% ovalbumin, and 0.5% Tween 20. YOL1/34 (Accurate Chemical & Scientific Corp., Westbury, NY) diluted 1:20 was used as a primary antitubulin antibody; rhodamine-conjugated rabbit anti-rat IgG (Miles-Yeda LTD) diluted 1:500 was used as a secondary antibody.

For immunofluorescence microscopy, imaging and analysis were performed using the DeltaVision Deconvolution System (Applied Precision Incorporated, Issaquah, WA) attached to an Olympus microscope with a Photometrix PXL Cooled CCD Camera. For visualizing the green fluorescent protein (GFP) fusions, exponentially growing cells were immobilized in low-melt agarose as described previously (Doyle and Botstein, 1996).

For 4′,6′-diamino-2-phenylindole (DAPI) staining of intracellular DNA, cells were poisoned by the addition of 1:30 volume of 1 M sodium azide to the medium and stained in PBS with 1 $\mu$g/ml DAPI for 10 min. Cells were observed and quantitated using a Zeiss axioscope.

For assessment of karyogamy, matings were performed by mixing together $10^8$ cells of each parent grown to exponential phase in YPD. Mixtures were pelleted, resuspended in 0.2 ml of YPD, spread on small YPD plates (35 × 10 mm, Falcon, Lincoln Park, NJ), and incubated for 3 to 4 h at 30°C. Subsequently, cells were washed off the plates and fixed in 3.7% formaldehyde or poisoned with sodium azide for immunofluorescent staining.

### *Overexpression of BIM1 from the GAL Promoter*

Strain DBY6654 transformed with pRB2652 or pTS161 was grown to exponential phase in minimal medium lacking uracil and containing 2% raffinose instead of glucose. Cells were centrifuged and resuspended in the same medium (control) or with 2% galactose instead of the raffinose. Cell density and viability were monitored; aliquots for immunofluorescence were removed at 10.5 h after induction.

## RESULTS

### *Bim1p Interacts with Tub1p in the Two-Hybrid System*

The two-hybrid system for detecting protein interactions in vivo (Fields and Sternglanz, 1994; Bai and Elledge, 1996) depends on the ability of proteins fused to the two essential domains of the *GAL4* transcription activator to interact well enough to restore *GAL4* function. Interaction is detected by observing the Gal4p-dependent expression of reporter genes (in our case *HIS3* and *Escherichia coli LacZ*) driven by the galactose promoter in the cell.

A two-hybrid screen was performed using the entire *TUB1* coding sequence (including the *TUB1* intron) fused to the DNA-binding domain of the *GAL4* gene; as described in detail above, this construct was made on a CEN plasmid carrying the *TRP1* gene. This plasmid (pRB2514) was introduced into a haploid strain Y190, selecting $Trp^+$ transformants. The bait plasmid-bearing strain was then transformed with a cDNA library fused to the *GAL4* activation domain (kindly provided by S. Elledge; cf. Amberg *et al.*, 1995a) carried on a 2-$\mu$m plasmid containing the *LEU2* gene. Among about 26,000 $Leu^+Trp^+$ transformants, 100 were found to be resistant to 50 mM aminotriazole (indicating *HIS3* function). Of these, 16 also expressed substantial levels of $\beta$-galactosidase. Among these, seven were eliminated by controls (most could activate the *LacZ* reporter gene independently of the bait plasmid).

The remaining library isolates were screened for the presence of *TUB2* as an insert by PCR, using one primer from the gene and one from the vector; two were detected. The remaining candidates were subjected to restriction mapping, and one representative of each restriction pattern was sequenced. Overall, we found 2 fusions to *TUB2* (encoding $\beta$-tubulin), 1 fusion to *BIK1*, 5 fusions in-frame to *BIM1* (YER016w), and 1 fusion in-frame to the last 20 residues of *ADH1* (this was not followed up further). The 5 *BIM1* candidates represented 4 instances of a fusion missing the first 70 residues and one instance of a fusion carrying essentially the entire coding sequence, missing only the first 9 residues.

To test whether *TUB3* will substitute for *TUB1* in binding *BIM1* in the two-hybrid system, a bait plasmid (pRB2639) was constructed in which the only difference from pRB2514 was the substitution of the tubulin gene sequences. Plasmid pRB2639 was tested for interaction by cotransformation as above with the longer *BIM1* clone. The resulting transformants both grew in the presence of 50 mM aminotriazole and produced $\beta$-galactosidase as well as control cotrans-

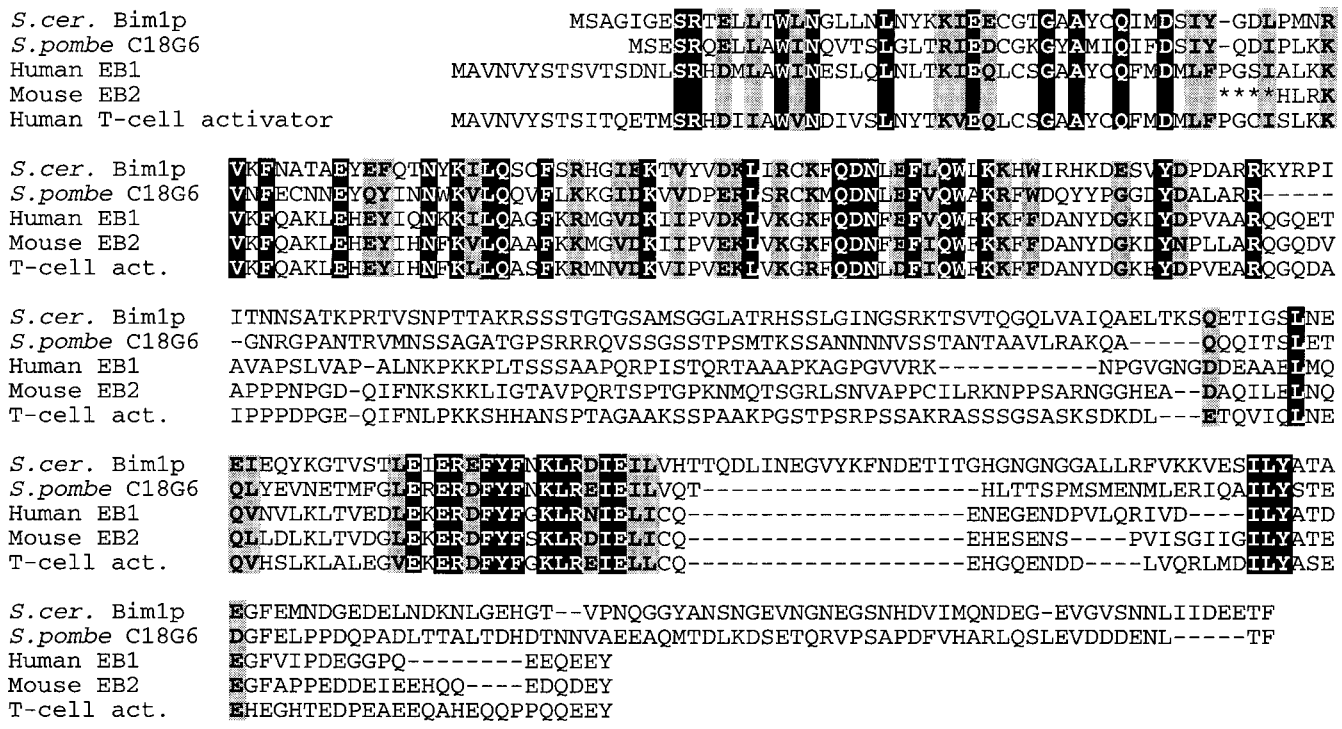


**Figure 1.** Modified FASTA alignment (Pearson and Lipman, 1988) of deduced amino acid sequences of completely sequenced homologues of *BIM1*. Identical residues are shown in black, similar ones in gray.

formants using pRB2514. Thus, Bim1p appears to be able to interact with either yeast α-tubulin.

Sequence alignment, using FASTA (Pearson and Lipman, 1988), of the predicted amino acid sequence of *BIM1* to several of its close homologues is shown in Figure 1. The protein is clearly well conserved over evolutionary time, with good homology (ca. 33–36% identity and ca. 56–61% similarity) to human, mouse and *S. pombe* (fission yeast). Blast searches of the EST databases (at NCBI, http://www.ncbi.nlm.nih.gov, July 6, 1997 release) revealed high-scoring homologues in *Drosophila*, *Caenorhabditis elegans*, zebra fish, and chicken (not shown). The best-characterized human homologue (EB1) was previously isolated in a two-hybrid screen using APC as bait (Su *et al.*, 1995). APC has been shown to bind microtubules (Munemitsu *et al.*, 1994; Smith *et al.*, 1994; Nathke *et al.*, 1996); the finding that an APC-binding molecule is homologous to a tubulin-binding molecule of yeast establishes a second connection between APC and microtubules.

### *Bim1p Colocalizes to Both Intranuclear and Extranuclear Microtubules*

The GFP of the jellyfish *Aequorea victoria* provides a convenient way to study subcellular localization of proteins in living cells (cf. Stearns, 1995). A variety of fusions of the *BIM1* coding sequence to GFP coding sequence were constructed (see MATERIALS AND METHODS). One of these, in which a mutant with increased fluorescence, S65T, (Heim *et al.*, 1995) of GFP is fused at the N terminus of Bim1p and driven by actin promoter, was introduced into wild-type cells and localization observed in a deconvolution fluorescence microscope system (DeltaVision). As the examples in Figure 2 illustrate, the GFP-Bim1p fusion protein colocalizes with both intranuclear and extranuclear (note especially panels I and J) microtubules. As shown below, this GFP-Bim1p fusion complements all of the growth phenotypes of *bim1*Δ mutants. It is possible that these conditions represent a mild overproduction if the *ACT1* promoter is significantly stronger than the *BIM1* promoter. Nevertheless, this experiment verifies directly that Bim1p localizes to the microtubule cytoskeleton, presumably by binding sites on α-tubulin.

### *Phenotypes of bim1Δ Mutants*

A *bim1* mutation that deletes the entire coding sequence was constructed by double-fusion PCR and introduced into a diploid strain. Upon tetrad dissection at 30°C, it was determined that haploid strains

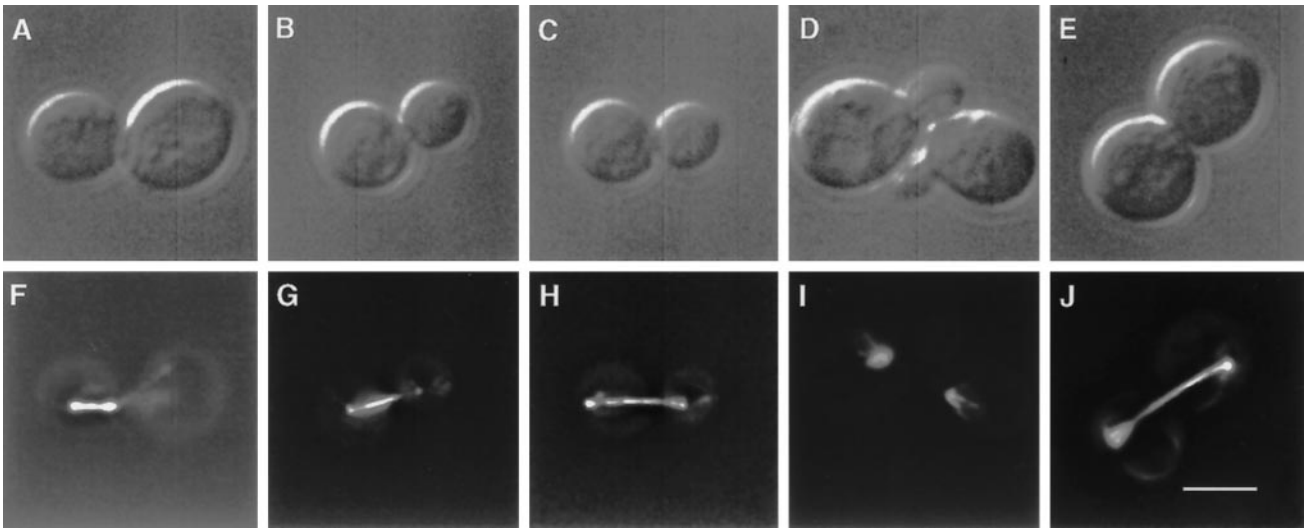


**Figure 2.** An N-terminal GFP-Bim1p fusion localizes to spindles and extranuclear microtubules. Nomarski (A–E) and FITC filter-illuminated (F–J) images capture different stages of cell cycle in strain DBY6654 transformed with pRB2654. Bar, 4 μm.

bearing the *bim1::URA3* allele are viable. Thereafter, the *bim1* deletion construct was introduced directly into haploid strains. Though viable, haploid strains with this mutation grow poorly at temperatures below 14°C and fail to grow at 37°C even though the parental strain grows up to 38°C. Significantly, *bim1*Δ strains fail to grow in concentrations of the antimicrotubule drug benomyl (i.e., 20 μg/ml) to which normal yeast are entirely resistant. These growth phenotypes are illustrated in Figure 3. Also shown in Figure 3 is the result that each of these growth phenotypes is completely complemented by the presence, on a low-copy plasmid, of the aforementioned GFP-Bim1p fusion driven by the *ACT1* promoter.

We examined haploid *bim1*Δ strains stained with antitubulin antibodies and DAPI using immunofluorescence microscopy in a DeltaVision deconvolution system. The images shown in Figure 4 are projections of several focal planes, included to show all of the staining, just as one would see if one focused up and down in a conventional fluorescence microscope. The examples of large-budded cells observed in the cultures shown in Figure 4 indicate that the spindles in *bim1*Δ mutants are short and/or misoriented even at permissive temperature (panels C and D show a cell in which the nucleus is dividing within the mother cell body). At 38°C (panels G-L; note the multibudded cell in panels I and J) nuclei appear to be undivided and the spindles are aberrant, being short and asymmetrically located between mother and daughter, as can be seen by comparing to the images of wild-type large budded cells (panels A, B, E, and F). No abnormal phenotype was observed in unbudded or small budded cells.

Quantitation of the nuclear migration and division defects is shown in Table 5. At nominally permissive temperature (i.e., 30°C), we found a significant increase (relative to wild type) in the frequency of improper nuclear migration (second and fifth columns). At low and high temperature the data are similar. There are also defects in nuclear division (columns 4 and 5) and in the frequency of binucleate mothers (column 2) at all temperatures. Despite the high frequency of these defects, viability of *bim1*Δ mutants

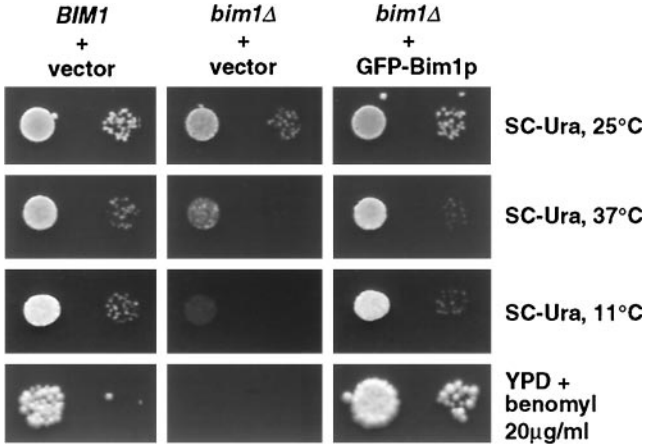


**Figure 3.** An N-terminal GFP-Bim1p fusion complements the heat and cold sensitive growth of the *bim1*Δ strain. Strains DBY6654 and DBY7305 transformed with vector pTS161 or plasmid pRB2654 were grown overnight in liquid minimal medium lacking uracil and then spotted as 1:10 and 1:1000 dilutions onto a YPD plate with benomyl added to a concentration of 20 μg/ml or onto minimal medium lacking uracil incubated at 25°C, 37°C, or 11°C.

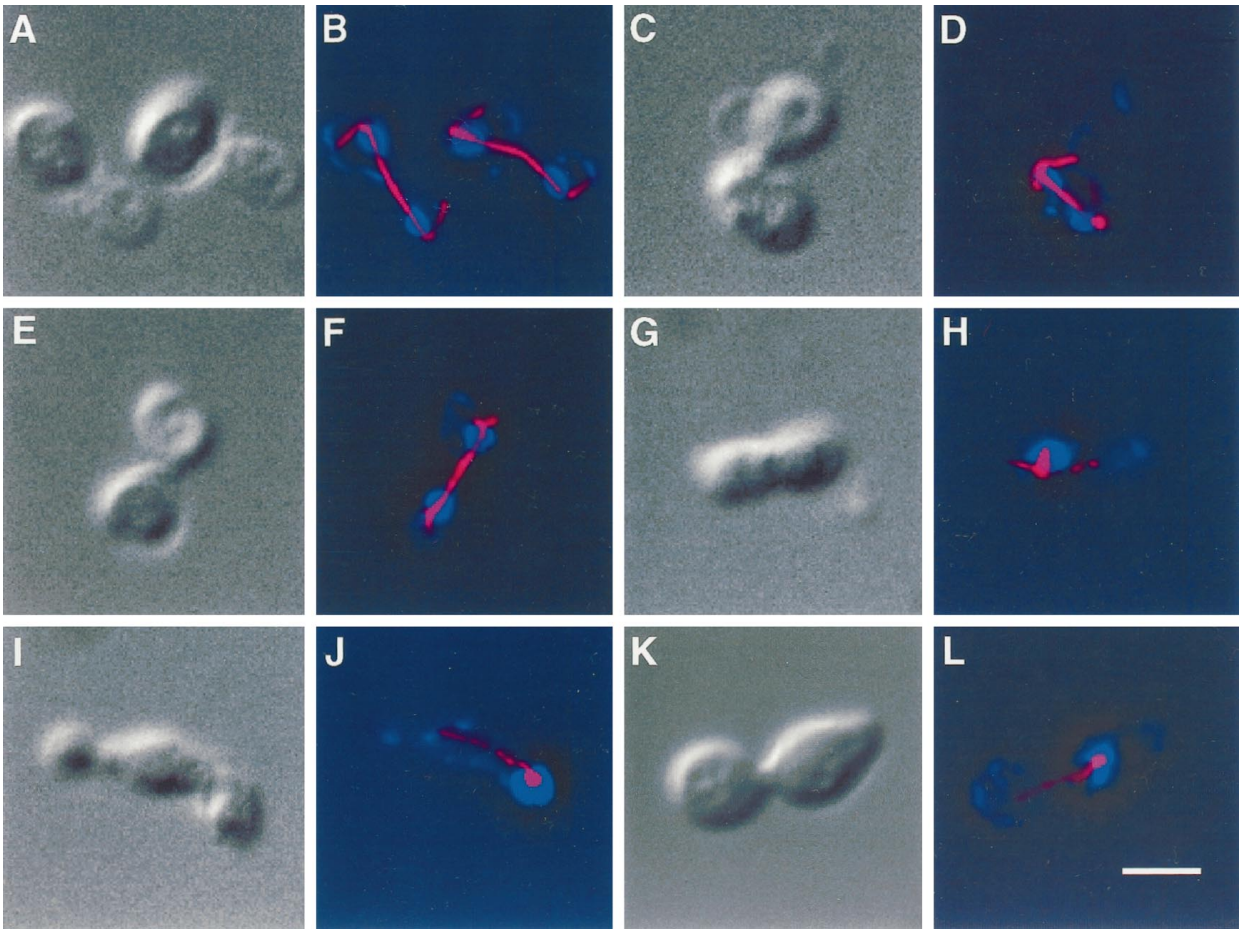


**Figure 4.** Microtubule morphology of *bim1*Δ at permissive and nonpermissive temperatures. The wild-type strain (DBY6654) grown at 30°C (A–B) or at 38°C (E–F) forms long spindles in large budded cells. The *bim1*Δ strain (DBY7305, C–D and G–L) exhibits a nuclear migration defect at 30°C (C–D) and spindle aberrations at 38°C (3.5 h after the shift, G–L). Nomarski images (A, C, E, G, I, and K) are shown next to combined images containing DAPI-stained nuclei and antitubulin-stained microtubules (B, D, F, H, J, and L). Bar, 4 μm.

after two generation times even at nonpermissive conditions is nearly normal; although after 24 h at the nonpermissive temperature (38°C), viability is decreased significantly (about sevenfold). Thus, we cannot account for the differential viability at extreme temperatures simply by the morphological changes we see.

**Table 5.** Nuclear morphology of large budded cells in *BIM1* and *bim1*Δ strains at different temperatures[a]

| Temperature (°C) | *BIM1* | *bim1*Δ | *BIM1* | *bim1*Δ | *BIM1* | *bim1*Δ | *BIM1* | *bim1*Δ | *BIM1* | *bim1*Δ |
|---|---|---|---|---|---|---|---|---|---|---|
| 12 | 85 | 42 | 2 | 15 | 0 | 13 | 12 | 15 | 1 | 15 |
| 30 | 85 | 35 | 0 | 14 | 0 | 1 | 14 | 33 | 1 | 17 |
| 38 | 73 | 20 | 2 | 6 | 5 | 1 | 15 | 44 | 4 | 29 |

[a] Strains DBY6654 (*BIM1*), DBY7303 (*bim1*Δ), and DBY7305 (*bim1*Δ) were grown at 30°C in YPD to exponential phase, shifted for two generation times to 12°C (24 h) or to 38°C (3.5 h), and stained with DAPI. Numbers shown are the percentage of large budded cells (always at least 100) counted. Data from two *bim1*Δ strains (DBY7303 and DBY7305) are similar and presented as an average.

**Table 6.** Nuclear morphology of zygotes[a]

| Strains | Fused nuclei | | | Unfused nuclei | | |
|---|---|---|---|---|---|---|
| | Unbudded | With bud | Total | Unbudded | With bud | Total |
| *wt* × *wt* | 41 | 27 | 68 | 32 | 0 | 32 |
| *bim1*Δ × *bim1*Δ | 1 | 0 | 1 | 53 | 46 | 99 |
| *wt* × *bim1*Δ | 41 | 37 | 78 | 21 | 1 | 22 |
| *bik1*Δ × *bik1*Δ | 3 | 17 | 20 | 58 | 22 | 80 |
| *wt* × *bik1*Δ | 30 | 36 | 66 | 32 | 2 | 34 |

[a] Strain DBY7305 was mated to DBY7303 (*bim1*Δ × *bim1*Δ) or to DBY6654 (*wt* × *bim1*Δ), strain DBY7831 was mated to DBY7835 (*bik1*Δ × *bik1*Δ) or to DBY6654 (*wt* × *bik1*Δ), and strain DBY7306 was mated to DBY6654 (*wt* × *wt*) as described in MATERIAL AND METHODS. After 4 h of mating, cells were washed off the plates and stained with DAPI. At least 100 zygotes were counted in each case, and numbers are shown as percentages.

### *Karyogamy Is Defective in the bim1Δ Mutant*

Failure of nuclear migration is characteristic of failure of extranuclear microtubule function (Huffaker *et al.*, 1988). Extranuclear microtubules are also implicated in karyogamy, the fusion of nuclei after mating. Many tubulin mutations exhibit a bilateral (i.e., both parents mutant) karyogamy failure, as do *bik1* mutants (Huffaker *et al.*, 1988; Berlin *et al.*, 1990; Richards, 1997). In preliminary tests we found that cells arising from micromanipulated *bim1*Δ × *bim1*Δ zygotes were rarely diploid, whereas from normal crosses such cells are regularly diploid. To quantitate the putative karyogamy defect, we carried out a mating experiment in which zygotes (which were equally abundant in all crosses we did) stained with DAPI were examined in the fluorescence microscope (Table 6). The data in Table 6 clearly show that both *bim1* and *bik1* (included as a control) mutants have bilateral karyogamy defects. Indeed, the *bim1* defect is even more striking than the *bik1* defect by this assay: whereas after 4 h, 80% *bik1* × *bik1* zygotes had unfused nuclei and 99% of *bim1* × *bim1* zygotes had unfused nuclei. The data also clearly show that Bim1p function in only one of the parents suffices to allow karyogamy.

Figure 5 shows immunofluorescence (DAPI and antitubulin staining) of zygotes that illustrates karyogamy failure at the level of the extranuclear microtubules, as in the *tub2* mutants and *bik1* mutants (Huffaker *et al.*, 1988; Berlin *et al.*, 1990). Unlike the extranuclear microtubules extending between the two nuclei in wild-type zygotes, in *bim1* × *bim1* zygotes the extranuclear microtubules are oriented at random.

### *Overexpression of BIM1 Results in Lethality and Cell Cycle Arrest*

To see whether Bim1p might interact stoichiometrically with tubulin (or another component of the mi-

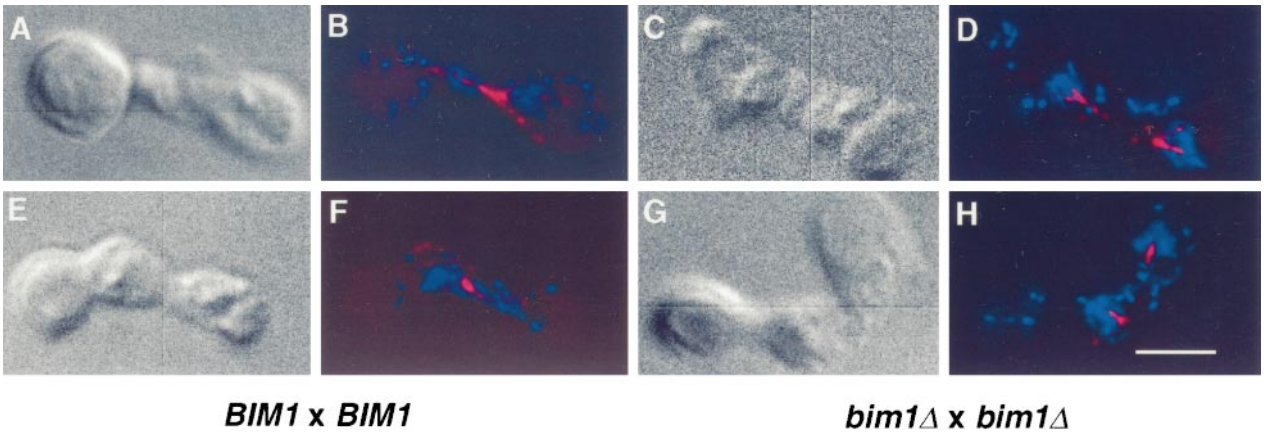


**Figure 5.** Microtubule and nuclear morphology in wild-type and mutant zygotes. Wild-type (DBY6654 × DBY7306, A–B and E–F) or *bim1*Δ strains (DBY7303 × DBY7305, C–D and G–H) were allowed to mate for 3 h and then were fixed for immunofluorescence. Nomarski images (A, C, E, and G) are shown next to combined images of DAPI-stained DNA and antitubulin-stained microtubules (B, D, F, and H). Bar, 4 μm.

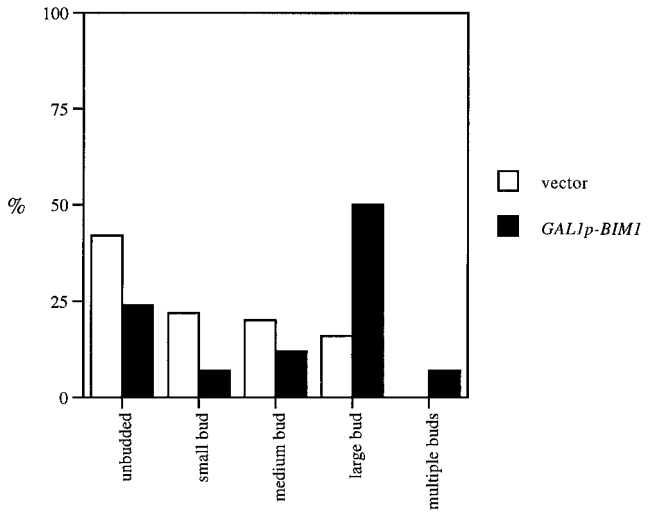


**Figure 6.** Overexpression of Bim1p causes accumulation of cells at the large budded stage. *GAL1* promoter-driven overexpression of Bim1p in strain DBY6654 transformed with pRB2652 was induced by growth in 2% galactose for 10.5 h. Columns reflect percentage of the cells counted (at least 200).

crotubule cytoskeleton), we arranged to overexpress *BIM1* from the *GAL1* promoter on a CEN plasmid; a similar plasmid with no insert was used as a control. Cells growing exponentially in raffinose medium were shifted into galactose medium. Whereas the control cells increased in number more than 10-fold (both cell numbers and viable cells) after 10 h in galactose, the cells overexpressing Bim1p grew only modestly (ca. twofold) in numbers and died, leaving less than 5% viable after 10 h. Despite the limitations imposed by this method (i.e., long induction times and use of a plasmid), the results are clearly indicative of microtubule function.

Figure 6 shows the cell cycle distribution in these cultures. It is clear that many of the cells overproducing *BIM1* have accumulated with a large bud. Table 7 shows quantitation documenting that after 10.5 h, virtually all of the large budded cells (ca. half the culture in the strain overproducing *BIM1*; Figure 6) are aberrant, in ways suggesting complete failure of nuclear division. These data also reveal impaired nuclear migration in cells overproducing *BIM1* similar to that seen in the *bim1*Δ mutants.

When the cells from this experiment were labeled with antitubulin antibodies and DAPI and examined in the DeltaVision fluorescence microscope, it emerged that the great majority of the large budded cells had arrested growth with an undivided nucleus, no spindle, and occasional long extranuclear microtubules (Figure 7). These results, though clearly more extreme, are reminiscent of the results found with *bim1*Δ mutants and indicate failure of the mitotic spindle.

**Table 7.** Nuclear morphology of large budded cells in a strain overexpressing *BIM1* from the *GAL1* promoter[a]

| |  |  |  |  |
|---|---|---|---|---|
| Vector | 98 | 2 | 0 | 0 |
| *GAL1p-BIM1* | 6 | 0 | 70 | 24 |

[a] Strain DBY6654 transformed with pRB2652 (GAL1p-BIM1) or pTS161 (vector) was grown in SC-Ura 2% raffinose to exponential phase and shifted to SC-Ura 2% galactose for 10.5 h. At least 100 large budded cells were counted from each culture. Numbers shown are the percentage of large budded cells counted.

### *Differential Interactions between Bim1p and Mutant α-Tubulins*

To carry out the various cellular functions in which microtubules are implicated, the tubulins must have a number of different ligands to which they can bind. It is likely that not all of these ligands bind tubulin in the same way. To study further the interactions between Bim1p and α-tubulin, we carried out two kinds of experiments. In one, we sought to find out whether there is a subset of *tub1* mutations that affect Bim1p binding in the two-hybrid system, essentially as done previously for ligands of actin (Amberg *et al.*, 1995a). In the other, we sought to discover overlapping of functions with individual *tub1* mutations by studying patterns of synthetic lethality and/or synthetic phenotype, as done previously for actin ligands (Holtzman *et al.*, 1994).

For both these purposes, we used a set of charged-to-alanine scanning mutations made in the *TUB1* gene (Richards, 1997). In the case of the two-hybrid differential interaction experiments, we replaced *TUB1* in the bait plasmid used to isolate *BIM1* with 51 mutant alleles (by PCR, in duplicate as described in MATERIALS AND METHODS). These plasmids were each examined to see whether the mutant Tub1p could interact with Bim1p and Bik1p to identify *tub1* alleles that showed differential interaction with either of the two ligands. Interaction was scored, as before, by assessment of growth on minimal medium plates supplemented with 50 mM 3-amino-1,2,4-triazole and confirmed by the β-galactosidase assay (an example of the growth data is given in Figure 8). The results (Table 8) were that only a limited number of *tub1* alleles failed to interact with Bik1p. The in vivo phenotypes of all of these *tub1* alleles are very severe; they are either recessive lethal or very growth impaired,

suggesting that lack of interaction may be due to gross structural defects in Tub1p.

The results with Bim1p are much more interesting. They recapitulate the differential interactions with Bik1p, but in addition, there are 11 *tub1* alleles that fail to interact with Bim1p but do interact with Bik1p. More encouragingly, six of the alleles that fail to interact with Bim1p are in a contiguous stretch on the primary sequence of the Tub1p (residues 393–432); of these, only one fails to interact with Bik1p. Absent a structure for tubulin, this is as good an indication as one could expect for a legitimate ligand-binding site.

In the case of the genetic differential interaction experiments, double mutants were made by crossing a *bim1*Δ mutant (DBY7301) to each of the viable *tub1* mutants. After tetrad dissection, the double mutants were identified by the segregation of auxotrophic markers: one (*ADE2*) marking the *bim1*Δ gene and the other (*LEU2*) tightly linked to the *tub1* mutation. Phenotypes were examined after loss of a wild-type *TUB1* plasmid which had been maintained to avoid any potential sporulation and/or germination defects resulting from the *tub1* mutation. The results (Table 8) show that only five *tub1* alleles are synthetically lethal with *bim1*Δ. Most significant is the observation that two of the five are among the six contiguous alleles that showed differential interactions in the two-hybrid assay. Furthermore, some of the other alleles in the contiguous stretch show a severe synthetic phenotype which is nearly, but not quite, lethal. These genetic and two-hybrid interaction results strongly reinforce each other, implicating this particular region of Tub1p in binding Bim1p.

### *Genetic Interactions between BIM1 and Other Components of the Microtubule Cytoskeleton*

To explore further the role of Bim1p in the function of the microtubule cytoskeleton, genetic interactions between *BIM1* and genes encoding other components of the microtubule cytoskeleton were examined. A *bim1*Δ mutant was crossed to a variety of mutants, including *tub2–201*, *num1*Δ, *bub3*Δ, and *bik1*Δ. These mutants were chosen because of their demonstrated genetic interactions with *TUB1*, implicating them either directly or indirectly in microtubule function. *TUB2* encodes β-tubulin, which is a component of the tubulin heterodimer (Neff *et al.*, 1983). Num1p localizes to the mother cell cortex, and *num1* mutants interact genetically with *tub1* and *tub2* mutants (Farkasovsky and Kuntzel, 1995). In addition, *num1* mutants have defects in nuclear migration (Kormanec *et al.*, 1991). Based on the localization of Num1p and the phenotype of *num1* mutants, *NUM1* is necessary for the proper function of cytoplasmic microtubules. *BUB3* encodes a protein which functions in the mitotic spindle assembly checkpoint (Hoyt *et al.*, 1991). Finally, as mentioned previously, the product of the *BIK1* gene, because of its phenotypes and localization to microtubules, is likely a structural component of the microtubule cytoskeleton (Berlin *et al.*, 1990).

Double mutants were made by crossing each of the mutants listed above to a *bim1*Δ mutant. Two diploids were made for each combination: one using a MAT**a** *bim1*Δ parent (DBY7303) and one using a MATα *bim1*Δ parent (DBY7301). In a combined total

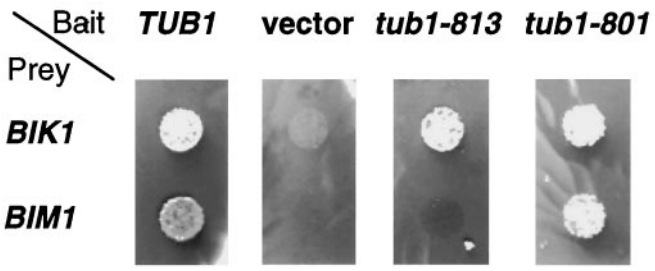


**Figure 8.** An example of differential interactions of *BIM1* and *BIK1* with *tub1* alleles. Strain Y190 was cotransformed with the indicated plasmids, grown in SC-Leu-Trp overnight and spotted onto minimal medium containing 10 μg/ml adenine and 50 mM 3-amino-1,2,4-triazole.

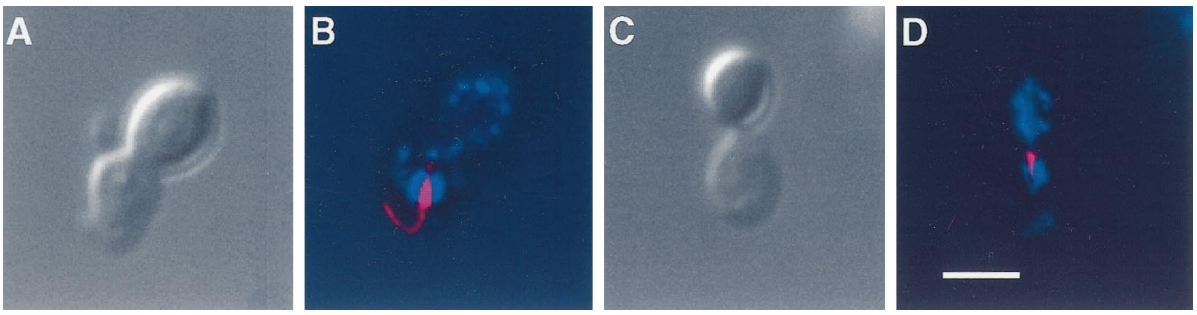


**Figure 7.** Overexpression of Bim1p causes arrest at the large budded stage with undivided nuclei. *GAL1* promoter-driven overexpression of Bim1p in DBY6654 transformed with pRB2652 was induced by growth in 2% galactose for 10.5 h. Nomarski images (A and C) are shown next to combined images of DAPI-stained DNA and antitubulin-stained microtubules (B and D). Bar, 4 μm.

**Table 8.** Differential genetic interactions of *tub1* alleles with *bim1*Δ compared to differential two-hybrid interactions with *BIM1* and *BIK1*[a]

| Allele | Phenotype | Genetic interaction with *bim1*Δ | 2-Hybrid interaction with BIM1p | 2-Hybrid interaction with Bik1p |
|---|---|---|---|---|
| *TUB1* | WT | | + | + |
| *tub1-801* | BenSS, cs, ts | SL | + | + |
| *tub1-802* | RL | ND | +/− | + |
| *tub1-803* | BenSS | SP | + | + |
| *tub1-804* | BenSS | None | + | + |
| *tub1-805* | BenSS | None | + | + |
| *tub1-806* | BenR | SP | + | + |
| *tub1-807* | BenSS | None | + | + |
| *tub1-808* | RL | ND | − | + |
| *tub1-809* | BenSS, slow | None | − | + |
| *tub1-810* | BenSS | None | + | + |
| *tub1-811* | WT | None | + | + |
| *tub1-812* | BenSS | SP | + | + |
| *tub1-813* | BenSS, cs, ts | SP | − | + |
| *tub1-814* | BenSS, slow | SS | − | − |
| *tub1-815* | WT | None | + | + |
| *tub1-816* | BenSS, cs | SP | + | + |
| *tub1-817* | BenSS | SP | + | + |
| *tub1-818* | BenSS, cs | SP | − | + |
| *tub1-819* | BenSS | None | + | + |
| *tub1-820* | DL | ND | Lethal | ND |
| *tub1-821* | BenSS | SP | − | + |
| *tub1-822* | BenSS, cs, ts | SP | + | + |
| *tub1-853* | BenSS, cs, ts | SL | + | + |
| *tub1-823* | RL | ND | − | − |
| *tub1-824* | BenSS, cs | SP | + | + |
| *tub1-825* | BenR | SP | + | + |
| *tub1-826* | BenR | SP | + | + |
| *tub1-827* | BenSS cs, ts | None | + | + |
| *tub1-828* | DL | ND | Lethal | ND |
| *tub1-829* | BenSS, cs, ts | SS | + | + |
| *tub1-830* | BenSS | SP | + | + |
| *tub1-831* | BenSS, cs | SL | − | + |
| *tub1-832* | BenR | SP | + | + |
| *tub1-833* | BenSS | None | + | + |
| *tub1-834* | BenSS, cs, ts | SS | − | − |
| *tub1-835* | WT | None | + | + |
| *tub1-836* | BenSS, cs, ts | SS | + | + |
| *tub1-837* | BenSS | None | + | + |
| *tub1-838* | BenSS | SP | + | + |
| *tub1-839* | BenR | None | + | + |
| *tub1-841* | BenR | SS | + | + |
| *tub1-842* | BenSS, cs, ts | SS | − | + |
| *tub1-845* | BenSS, cs, ts | SP | − | − |
| *tub1-846* | BenSS, cs, ts | SL | − | + |
| *tub1-847* | BenSS, cs, ts | SS | − | + |
| *tub1-848* | BenSS, cs, ts | SL | − | +/− |
| *tub1-849* | BenSS, cs, ts | SS | − | + |
| *tub1-850* | BenSS | SP | + | + |
| *tub1-851* | BenSS | None | + | + |
| *tub1-852* | BenSS | SP | + | + |

[a] *tub1* alleles are listed in 5′ to 3′ order in the first column. The phenotype resulting from each *tub1* allele alone is shown in the second column (WT, wild-type; DL, dominant lethal; RL, recessive lethal; BenSS, benomyl-supersensitive; cs, cold-sensitive; ts, heat-sensitive; slow, poor growth at all temperatures). The third column shows the effects of combining each *tub1* allele with *bim1*Δ (none, no synthetic phenotype; SP, synthetic phenotype; SS, synthetic "sickness"; SL, synthetic lethality; ND, not done). Columns 4 and 5 show the results of testing two-hybrid interactions of the *tub1* alleles with *BIM1* and *BIK1*, respectively. Strains obtained by cotransforming Y190 with various combinations of bait plasmids and library isolates containing *BIK1* or *BIM1* fused to the *GAL4* activation domain were spotted on SD + 10 μg/ml adenine and 50 mM 3-amino-1,2,4-triazole. Interaction was scored as +, robust growth; +/−, intermediate growth; or −, poor or no growth.

**Table 9.** Synthetic lethality between null alleles of several microtubule cytoskeleton components[a]

| | Inferred double mutants | Observed double mutants | p |
|---|---|---|---|
| *bim1*Δ × *num1*Δ | 8 | 0 | 0.005 |
| *bim1*Δ × *bub3*Δ | 18 | 0 | 0.00002 |
| *bim1*Δ × *bik1*Δ | 8 | 0 | 0.005 |
| *bim1*Δ × *tub2-201* | 6 | 6 | n/a |
| *bik1*Δ × *bub3*Δ | 16 | 0 | 0.00006 |

[a] Crosses between various mutants in microtubule cytoskeleton components (*bim1*Δ, *bik1*Δ, *num1*Δ, *bub3*Δ, and *tub2-201*) were performed as described in MATERIALS AND METHODS, and the resulting tetrads (at least 20 for each combination) were sporulated and dissected. Data from all crosses which failed to yield viable double mutants are shown. Only information from nonparental ditype tetrads is shown, because in those tetrads identification of the double mutants by the auxotrophic markers which marked each deletion was unambiguous, even when the two disruptions were marked by the same auxotropy. The number of double mutants dissected from nonparental ditype tetrads is shown in "Inferred double mutants" whereas the number of these spores which formed colonies is shown in "Observed double mutants." The p value is the result of a $\chi^2$ test using the null hypothesis that in the nonparental ditype tetrads, the 50% viability observed is randomly distributed. In all cases, except with *bim1*Δ × *tub2-201*, included as an example of a cross from which viable double mutants were recovered, there is significant deviation from the distribution predicted by the null hypothesis, suggesting that the lethality is caused by the double-mutant genotype.

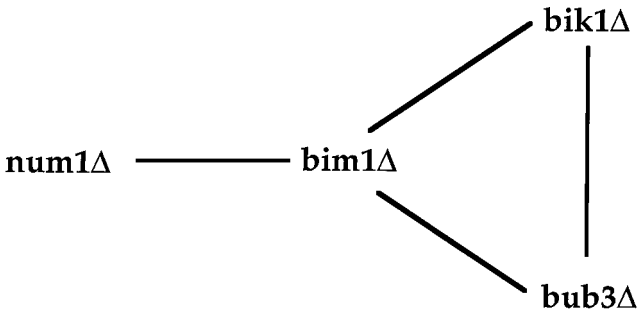


**Figure 9.** Synthetic lethal interactions between null alleles of genes encoding components of the microtubule cytoskeleton. Single mutants (*bim1*Δ, *bik1*Δ, *bub3*Δ, *num1*Δ, and *tub2–201*) were crossed in all pairwise combinations as described in MATERIALS AND METHODS, and diploids were dissected to obtain double mutants. In the combinations connected by a line, no double mutants were recovered, indicating synthetic lethality between the two mutations. In all other combinations, viable double mutants were recovered.

of 20 tetrads dissected from both crosses, double mutants containing *bim1*Δ and either *num1*Δ, *bik1*Δ, or *bub3*Δ were never observed. This lack of double mutants is statistically significant in all three cases (Table 9). On the other hand, *tub2–201 bim1*Δ double mutants are viable. Therefore, *bim1*Δ is synthetically lethal with *num1*Δ, *bik1*Δ, and *bub3*Δ, indicating possible redundancy of functions between Bim1p and these gene products.

All other pairwise combinations of these mutants were also tested for viability in a similar manner. The only other cross from which double mutants failed to be recovered was *bik1*Δ × *bub3*Δ; the statistical significance of this lack of viable double mutants is also shown in Table 9. The synthetic lethal interactions among these microtubule cytoskeleton components are diagrammed in Figure 9. It is notable that while *bim1*Δ is synthetically lethal with *num1*Δ, *bik1*Δ shows no such effects; indeed, the growth of the *bik1*Δ *num1*Δ strain is not more impaired under any condition (including growth on benomyl) relative to either of the two parental strains.

## DISCUSSION

All of the data presented above support the identification of the *BIM1* gene (*YER016w*) as a structural component of the microtubule cytoskeleton of *S. cerevisiae*. Most of the observations closely resemble similar published data on the genes encoding the tubulin subunits themselves as well as bona fide microtubule-associated genes in yeast (Botstein *et al.*, 1997). The essential observations include binding in the two-hybrid system, colocalization with microtubules, characteristic phenotypes of the viable null *bim1* mutants, overexpression lethality resulting in complete spindle failure, and specific genetic interactions (synthetic lethality) not only with a subset of *tub1* alleles but also with a variety of other genes associated with the microtubule cytoskeleton.

Even though the data for a physical interaction between Bim1p and Tub1p is very strong, we cannot absolutely rule out the possibility that the interaction involves other proteins, although there is little precedent for the kind of allele-specific effects we observe in truly indirect interactions. Final proof will no doubt require an in vitro system capable of assessing assembly and/or function of microtubules.

The original two-hybrid screen yielded, in addition to *BIM1*, two other genes, *BIK1* and *TUB2*. Both of these genes have been studied quite extensively, and mutants in each have features resembling those of *bim1* mutants. Notable among these are the failures in karyogamy and nuclear migration, both associated with functional failure or absence of extranuclear microtubules.

The many similarities and few differences between *BIM1* and *BIK1* are instructive. Among the similarities are viable null phenotype, hypersensitivity to benomyl, karyogamy failure, nuclear migration, and spindle defects, and, most important, overexpression lethality resulting in spindle failure. The last observation, in particular, is significant in that it suggests, for Bim1p as it did for Bik1p, that it is "required

stoichiometrically for the formation or stabilization of microtubules" (Berlin *et al.*, 1990); see also Rose and Fink, 1987). Indeed, the observation of synthetic lethality between *bim1* and *bik1* null mutants supports their role in a similar or shared function.

The differences between the *bim1* and *bik1* null phenotypes may hold some clues as to some differentiation in function. First, the karyogamy failure of *bim1* mutants in our hands is more severe than contemporaneous *bik1* controls. Second, the *BIM1* overexpression effects on nuclear migration are more severe than those reported for *BIK1* (Berlin *et al.*, 1990). Since nuclear migration and karyogamy both are effected by extranuclear microtubules, it is tempting to speculate that the two genes have largely overlapping functions, but that *BIM1* is more critical for extranuclear microtubule function. In support of this idea is the pattern of synthetic lethality: *bim1* null mutations show synthetic lethality with *num1* null mutations whereas the *bik1* null mutation does not. The *NUM1* function is clearly associated with extranuclear and not intranuclear microtubule function (Farkasovsky and Kuntzel, 1995). Nevertheless, *BIM1* seems also to be involved with spindle function, given the decreased number of long spindles in the *bim1*Δ mutant and the synthetic lethality between *bim1*Δ and *bub3*Δ, a gene that functions in the spindle assembly checkpoint.

We describe an attempt to define, within the Tub1p sequence, the regions important for interactions between α-tubulin and Bim1p and Bik1p. Although in the case of Bik1p, we could conclude little, as we found few specific interactions, the case of Bim1p was much more encouraging. Indeed our results predict that a region near the C terminus of Tub1p is the locus of interaction between it and Bim1p. We look forward to the time that molecular structures of microtubules become available so that this kind of prediction can be validated, as was the case for similar experiments with yeast actin (Amberg *et al.*, 1995a).

The interpretation of the observation that alanine-scanning mutations in similar regions of Tub1p display both synthetic lethality and differential interaction in the two-hybrid system is not straightforward. Using the reasoning of Holtzman *et al.* (1994), mutations that fail to interact with a ligand should not be exacerbated by total loss of the otherwise dispensable ligand. We are obliged, therefore, to propose instead that the differential interactions are not a sign of complete loss of binding affinity. Instead, we imagine that each of the many mutations that we can detect as different in the assay provide only a fraction of the binding energy, so that only an ensemble of many alanine-scanning alleles would result in complete failure of binding in vivo. Furthermore, synthetic lethality between these *tub1* alleles and *bim1*Δ implies redundancy of function; one possible explanation is that both Bim1p and this subset of *tub1* alleles cooperate to recruit another essential ligand to microtubules.

Finally, we return to the homology between Bim1p and its mammalian homologues. Human EB1 protein, the nearest homologue to Bim1p, was recovered in a two-hybrid screen as a ligand of APC, the gene responsible for a hereditary predisposition to a form of colon cancer (Groden *et al.*, 1991; Su *et al.*, 1995). It is APC itself (which has no close homologue in the yeast genome), and not EB1, that has been shown to bind microtubules (Munemitsu *et al.*, 1994; Smith *et al.*, 1994). EB1 has not, to our knowledge, yet been tested for microtubule binding. Our results provide a second line of evidence linking APC and microtubules, since our data suggest that EB1 itself may well bind to microtubules. The fact that there is no close APC homologue in yeast suggests that it is EB1/Bim1p, and not APC, that is the highly conserved structural component common to all eukaryotic genera (supported by the widespread occurrence of Bim1p homologues in a variety of diverse organisms).

To conclude, we have found that yeast *BIM1* encodes a protein likely to be a structural component of the yeast microtubule cytoskeleton. The similarity to human EB1, along with the additional microtubule association via APC, suggests that EB1 is likewise a structural component of the mammalian microtubule cytoskeleton, thus providing a framework for the understanding of the functions of microtubules in both systems.

## ACKNOWLEDGMENTS

We thank Steve Elledge for λYES cDNA library; Tim Stearns for useful discussions and advice; Koustubh Ranade, Craig Cummings, and Tracy Ferea for critical reading of the manuscript; and Susan Palmieri and Chris Kenfield for assistance with DeltaVision deconvolution system. This work was supported by a grant from the National Institutes of Health (GM-46406).

## REFERENCES

Amberg, D.C., Basart, E., and Botstein, D. (1995). Defining protein interactions with yeast actin in vivo. Nat. Struct. Biol. *2*, 28–35.

Amberg, D.C., Botstein, D., and Beasley, E.M. (1995). Precise gene disruption in *Saccharomyces cerevisiae* by double fusion polymerase chain reaction. Yeast *11*, 1275–1280.

Bai, C., and Elledge, S.J. (1996). Gene identification using the yeast two-hybrid system. Methods Enzymol. *273*, 331–347.

Barnes, G., Louie, K.A., and Botstein, D. (1992). Yeast proteins associated with microtubules in vitro and in vivo. Mol. Biol Cell. *3*, 29–47.

Berlin, V., Styles, C.A., and Fink, G.R. (1990). BIK1, a protein required for microtubule function during mating and mitosis in *Saccharomyces cerevisiae*, colocalizes with tubulin. J. Cell Biol. *111*, 2573–2586.

Botstein, D., Amberg, A., Mulholland, J., Huffaker, T., Adams, A., Drubin, D., and Stearns, T. (1997). The yeast cytoskeleton. In: The Molecular and Cellular Biology of the Yeast *Saccharomyces*, ed. J.

Pringle, J. Broach, and E. Jones, Cold Spring Harbor, NY: Cold Spring Harbor Laboratory Press, 1–90.

Byers, B. (1981). Cytology of the yeast life cycle. In: The Molecular Biology of the Yeast *Saccharomyces*, ed. J.N. Strathern, E.W. Jones, and J.R. Broach, Cold Spring Harbor, NY: Cold Spring Harbor Laboratory Press, 59–96.

Doyle, T., and Botstein, D. (1996). Movement of yeast cortical actin cytoskeleton visualized in vivo. Proc. Natl. Acad. Sci. USA *93*, 3886–3891.

Farkasovsky, M., and Kuntzel, H. (1995). Yeast Num1p associates with the mother cell cortex during $S/G_2$ phase and affects microtubular functions. J. Cell Biol. *131*, 1003–14.

Fields, S., and Sternglanz, R. (1994). The two-hybrid system: an assay for protein–protein interactions. Trends Genet. *10*, 286–292.

Groden, J., Thliveris, A., Samowitz, W., *et al.* (1991). Identification and characterization of the familial adenomatous polyposis coli gene. Cell *66*, 589–600.

Guthrie, C., and Fink, G.R. (1991). Guide to yeast genetics and molecular biology. Methods Enzymol. *194*, passim.

Harlow, E., and Lane, D.P. (1988). Antibodies: A Laboratory Manual, Cold Spring Harbor, NY: Cold Spring Harbor Laboratory Press.

Heim, R., Cubitt, A.B., and Tsien, R.Y. (1995). Improved green fluorescence (Letter). Nature *373*, 663–664.

Holtzman, D.A., Wertman, K.F., and Drubin, D.G. (1994). Mapping actin surfaces required for functional interactions in vivo. J. Cell Biol. *126*, 423–432.

Hoyt, M.A., He, L., Loo, K.K., and Saunders, W.S. (1992). Two *Saccharomyces cerevisiae* kinesin-related gene products required for mitotic spindle assembly. J. Cell Biol. *118*, 109–20.

Hoyt, M.A., Totis, L., and Roberts, B.T. (1991). *S. cerevisiae* genes required for cell cycle arrest in response to loss of microtubule function. Cell *66*, 507–517.

Huffaker, T.C., Thomas, J.H., and Botstein, D. (1988). Diverse effects of beta-tubulin mutations on microtubule formation and function. J. Cell Biol. *106*, 1997–2010.

Interthal, H., Bellocq, C., Bahler, J., Bashkirov, V.I., Edelstein, S., and Heyer, W.D. (1995). A role of Sep1 (= Kem1, Xrn1) as a microtubule-associated protein in *Saccharomyces cerevisiae*. EMBO J. *14*, 1057–1066.

Irminger-Finger, I., Hurt, E., Roebuck, A., Collart, M.A., and Edelstein, S.J. (1996). MHP1, an essential gene in *Saccharomyces cerevisiae* required for microtubule function. J. Cell Biol. *135*, 1323–1339.

Ito, H., Fukuda, Y., Murata, K., and Kimura, A. (1983). Transformation of intact yeast cells treated with alkali cations. J. Bacteriol. *153*, 163–168.

Jones, J.S., and Prakash, L. (1990). Yeast *Saccharomyces cerevisiae* selectable markers in pUC18 polylinkers. Yeast *6*, 363–366.

Kilmartin, J.V., and Adams, A.E. (1984). Structural rearrangements of tubulin and actin during the cell cycle of the yeast Saccharomyces. J. Cell Biol. *98*, 922–933.

Kormanec, J., Schaaff, G.I., Zimmermann, F.K., Perecko, D., and Kuntzel, H. (1991). Nuclear migration in *Saccharomyces cerevisiae* is controlled by the highly repetitive 313 kDa NUM1 protein. Mol. Gen. Genet. *230*, 277–287.

Meluh, P.B., and Rose, M.D. (1990). KAR3, a kinesin-related gene required for yeast nuclear fusion (published erratum appears in Cell *61*, 548, 1990. Cell *60*, 1029–1041.

Munemitsu, S., Souza, B., Muller, O., Albert, I., Rubinfeld, B., and Polakis, P. (1994). The APC gene product associates with microtubules in vivo and promotes their assembly in vitro. Cancer Res. *54*, 3676–3681.

Nathke, I.S., Adams, C.L., Polakis, P., Sellin, J.H., and Nelson, W.J. (1996). The adenomatous polyposis coli tumor suppressor protein localizes to plasma membrane sites involved in active cell migration. J. Cell Biol. *134*, 165–179.

Neff, N.F., Thomas, J.H., Grisafi, P., and Botstein, D. (1983). Isolation of the beta-tubulin gene from yeast and demonstration of its essential function in vivo. Cell *33*, 211–219.

Pasqualone, D., and Huffaker, T.C. (1994). STU1, a suppressor of a beta-tubulin mutation, encodes a novel and essential component of the yeast mitotic spindle. J. Cell Biol. *127*, 1973–1984.

Pearson, W.R., and Lipman, D.J. (1988). Improved tools for biological sequence comparison. Proc. Natl. Acad. Sci. USA *85*, 2444–2448.

Pellman, D., Bagget, M., Tu, H., and Fink, G.R. (1995). Two microtubule-associated proteins required for anaphase spindle movement in *Saccharomyces cerevisiae*. J. Cell Biol. *130*, 1373–1385.

Richards, K. (1997). Genetic analysis of the *TUB1* gene in *Saccharomyces cerevisiae*. Genetics, Stanford: Stanford University.

Roof, D.M., Meluh, P.B., and Rose, M.D. (1992). Kinesin-related proteins required for assembly of the mitotic spindle. J. Cell Biol. *118*, 95–108.

Rose, M.D., and Fink, G.R. (1987). KAR1, a gene required for function of both intranuclear and extranuclear microtubules in yeast. Cell *48*, 1047–1060.

Sambrook, J., Fritsch, E.F., and Maniatis, T. (1989). Molecular Cloning: A Laboratory Manual, 2nd ed., Cold Spring Harbor, NY: Cold Spring Harbor Laboratory Press.

Schatz, P.J., Solomon, F., and Botstein, D. (1986). Genetically essential and nonessential alpha-tubulin genes specify functionally interchangeable proteins. Mol. Cell. Biol. *6*, 3722–3733.

Schatz, P.J., Solomon, F., and Botstein, D. (1988). Isolation and characterization of conditional-lethal mutations in the TUB1 alpha-tubulin gene of the yeast *Saccharomyces cerevisiae*. Genetics *120*, 681–695.

Smith, K.J., Levy, D.B., Maupin, P., Pollard, T.D., Vogelstein, B., and Kinzler, K.W. (1994). Wild-type but not mutant APC associates with the microtubule cytoskeleton. Cancer Res. *54*, 3672–3675.

Stearns, T. (1995). Green fluorescent protein. The green revolution. Curr. Biol. *5*, 262–264.

Stotz, A., and Linder, P. (1990). The ADE2 gene from *Saccharomyces cerevisiae*: sequence and new vectors. Gene *95*, 91–98.

Su, L.K., Burrell, M., Hill, D.E., Gyuris, J., Brent, R., Wiltshire, R., Trent, J., Vogelstein, B., and Kinzler, K.W. (1995). APC binds to the novel protein EB1. Cancer Res. *55*, 2972–2977.

Trueheart, J., Boeke, J.D., and Fink, G.R. (1987). Two genes required for cell fusion during yeast conjugation: evidence for a pheromone-induced surface protein. Mol. Cell. Biol. *7*, 2316–2328.

Yaffe, M.P., Ohta, S., and Schatz, G. (1985). A yeast mutant temperature-sensitive for mitochondrial assembly is deficient in a mitochondrial protease activity that cleaves imported precursor polypeptides. EMBO J. *4*, 2069–2074.